ORGANOMETALLICS

Tutorial

Cite This: *Organometallics* 2018, 37, 505−516

# Activation of Carbon−Hydrogen Bonds via 1,2-RH-Addition/-Elimination to Early Transition Metal Imides

Peter T. Wolczanski*

Department of Chemistry & Chemical Biology, Baker Laboratory, Cornell University, Ithaca, New York 14853, United States

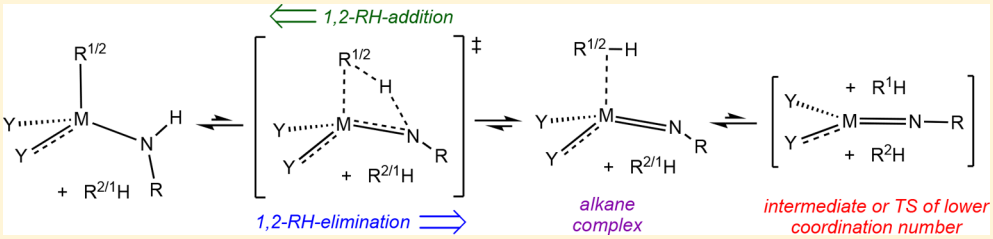


**ABSTRACT:** A tutorial addressing the activation of carbon−hydrogen bonds via the 1,2-RH-addition to high oxidation state, early metal $X_nM{=}NR$ complexes is described. Details regarding the reverse 1,2-RH-elimination from $X_n(R')M{-}NHR$, are also presented. The overall process is discussed as follows: (1) electrophilicity and electronics; (2) general mechanism; (3) kinetics of 1,2-RH-elimination; (4) periodic trends; (5) alkane complexes; (6) kinetic isotope effects (KIEs); (7) RH activation selectivities; and (8) future directions.

## INTRODUCTION

At an American Chemical Society Meeting in Toronto in 1988, the activation of hydrocarbons by zirconium imido functionalities, or 1,2-RH-addition, was independently reported by two groups: Christopher "Kit" C. Cummins and Peter T. Wolczanski (P.T.W.) at Cornell University and Robert G. Bergman (R.G.B.) and Patrick J. Walsh at the University of California, Berkeley.[1,2] Concurrent publications initially resulted from the discovery,[3,4] and significant differences in the respective systems permitted the prolonged investigation of 1,2-RH-addition/elimination by both groups with minimal interference, great scientific discourse, and a lot of enjoyable chemistry. While this tutorial will be biased toward the research conducted in the PTW laboratories given its author, investigations by both groups and later contributors have provided crucial input to the understanding of the process.

Scheme 1 provides a sample of the initial discoveries of 1,2-RH-addition to transient imido species discovered at Cornell. Thermolysis of $(^tBu_3SiNH)_3ZrR$ (**1**-R; R = $^c$Hex, Me) induced the 1,2-RH-elimination of $^c$HexH and MeH, respectively, to produce the putative intermediate three-coordinate imide $(^tBu_3SiNH)_2Zr{=}NSi^tBu_3$ (**2**), which adds a variety of hydrocarbons via 1,2-RH-addition, including aromatics such as benzene, and those containing $sp^3$-CH bonds. For example, thermolysis of **1**-$^c$Hex in the presence of excess methane in $C_6D_{12}$ afforded **1**-Me in quantitative yield. Transient imide **2** was also trapped with dihydrogen to provide the hydride $(^tBu_3SiNH)_3ZrH$ (**1**-H) and by THF to generate the adduct $(^tBu_3SiNH)_2(^tBu_3SiN{=})Zr(THF)$ (**2**-THF).

While the corresponding $Cp_2Zr{=}NR$ system investigated at Berkeley was initially limited to aromatics in its CH activation chemistry, a diverse set of imido reactivity was explored. As Scheme 2 elaborates, thermolyses of $Cp_2Zr(NHR)Me$ (R = $^t$Bu, **3**-Me) or $Cp_2Zr(NHR)_2$ (R = $^t$Bu, **4**-N$^t$Bu) provided the related transient imido complex, $Cp_2Zr{=}N^tBu$ (**5**), which added benzene to produce $Cp_2Zr(NH^tBu)Ph$ (**3**-Ph), or was trapped by THF to afford the adduct, $Cp_2Zr(=N^tBu)(THF)$ (**5**-THF). A different trapping agent, 1-phenyl-propyne, underwent a 2 + 2 cyclization with the imide to afford the regioselective azametalacyclobutene species, $Cp_2Zr(\kappa$-N,C-N-

**Scheme 1. Discovery of 1,2-RH-Addition in the $(^tBu_3SiNH)_3ZrR$ (1-R) System**

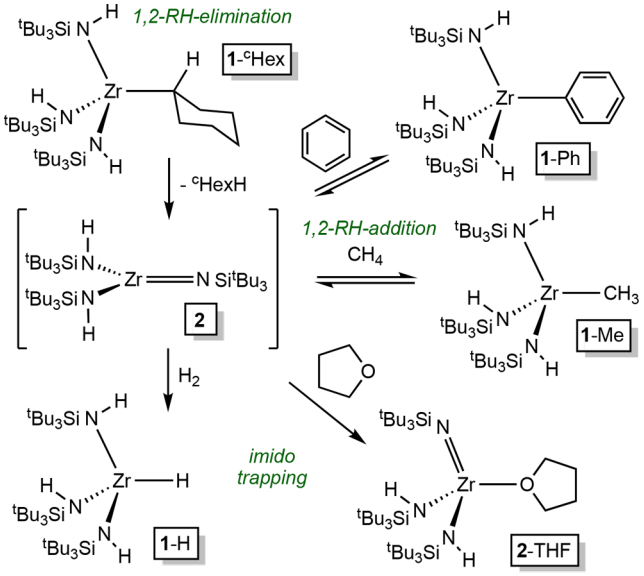


**Received:** October 10, 2017
**Published:** February 5, 2018




DOI: 10.1021/acs.organomet.7b00753
*Organometallics* 2018, 37, 505−516

**Scheme 2. Reactivity, Including 1,2-PhH-Addition, of the $Cp_2Zr{=}NR$ System**

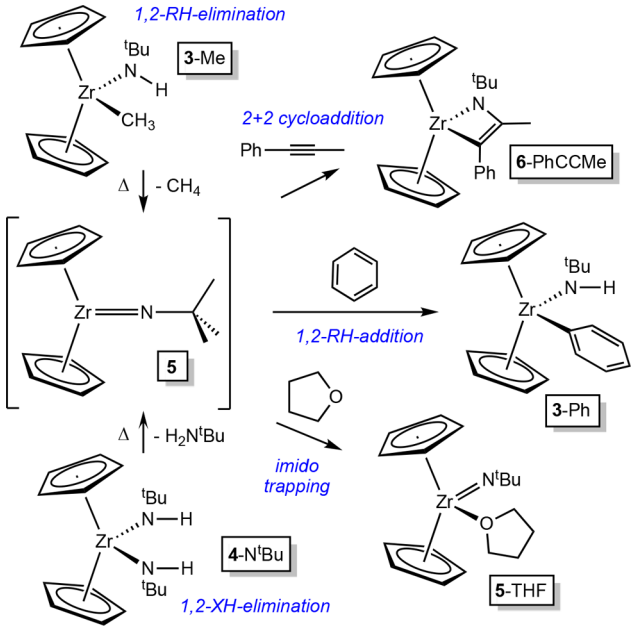


($^t$Bu)CMe=CPh) (**6**-PhCCMe), whose constituents indicated an anti-Markovnikov process.

The focus of this tutorial is the 1,2-RH-addition/elimination of hydrocarbons to early transition metal imides, but there are related reactions by other metal-element multiple bonds. Most abstraction processes can be construed as 1,2-RH-eliminations, such as those initiated by Schrock[5,6] to synthesize $d^0$ alkylidenes. Some abstractions, which have been addressed mechanistically by Zue,[7] are irreversible, but there are cases in which transient $L_nM{=}CHR$ species add CH bonds,[8−11] including a limited number of intermolecular cases.[12−16] Mindiola has observed reversibility in the addition of RH to metal alkylidynes, and examples of this remarkable chemistry are illustrated in Scheme 3.[17−21]

An abstraction to form a titanium neopentylidyne occurs via thermolysis of a neopentylidene-neopentyl complex, and various hydrocarbons have been shown to add across the multiple bond.[18,19] MeH and primary hydrocarbons undergo 1,2-RH-addition, and these processes are coupled with hydrogen migrations from the $\alpha$- or $\beta$-positions of the alkyl derived from activation. In the case of alkyls with $\beta$-hydrogens, the bound olefin, portrayed in Scheme 3 as a metallacyclopropane, can be released upon addition of $N_2O$ or $N_3R'$ (R′ = Ad (adamantyl), $SiMe_3$).[19] Methane activation leads to a methyl complex, and it is in equilibrium with a methylidene derivative via H-migration.[20]

## THE TUTORIAL

**Electrophilicity and Electronics.** A common feature critical to the activation of CH-bonds by $(^tBu_3SiNH)_2Zr{=}NSi^tBu_3$ (**2**) and $Cp_2Zr{=}N^tBu$ (**5**) via 1,2-RH-addition is a localized electrophilic site. While there are numerous transition metal imido species in groups 4−6, those whose electrophilic character is dispersed about the metal manifest no CH-bond activation activity. From the perspective of electron counting,[22] with $RNH^-$ and $RN^{2-}$ as 4- and 6-electron donors, respectively, to $d^0$ Zr(IV), **2** is at most a 14-electron compound while **5** is accorded 16 electrons.[23,24] The two cyclopentadienide rings of **5** each donate 6 electrons, but the $RN^{2-}$ is constrained to $\pi$-donate only in the $Cp_2Zr$ "wedge"[25] and is limited to being a 4-electron donor as a consequence.

As Figure 1 illustrates, empty orbitals on $(^tBu_3SiNH)_2Zr{=}NSi^tBu_3$ (**2**)[23,24] and $Cp_2Zr{=}N^tBu$ (**5**)[25] that are best construed as $d_{z^2}$ serve as the initial receptors of the pair of electrons in a carbon−hydrogen bond. The additional steric constraints imposed by the diamide and dicyclopentadienyl units help orient the substrate for activation by aligning the R−H bond along the M=N axis. Since the transfer of an R group to the imide nitrogen within a four-center TS has never been established, only the configuration with H oriented toward the

**Scheme 3. 1,2-PhH-Addition in the Transient Alkylidyne $\{(2\text{-}PPh_2,4\text{-}Me\text{-}C_6H_3)_2N\}TiC^tBu$ System**

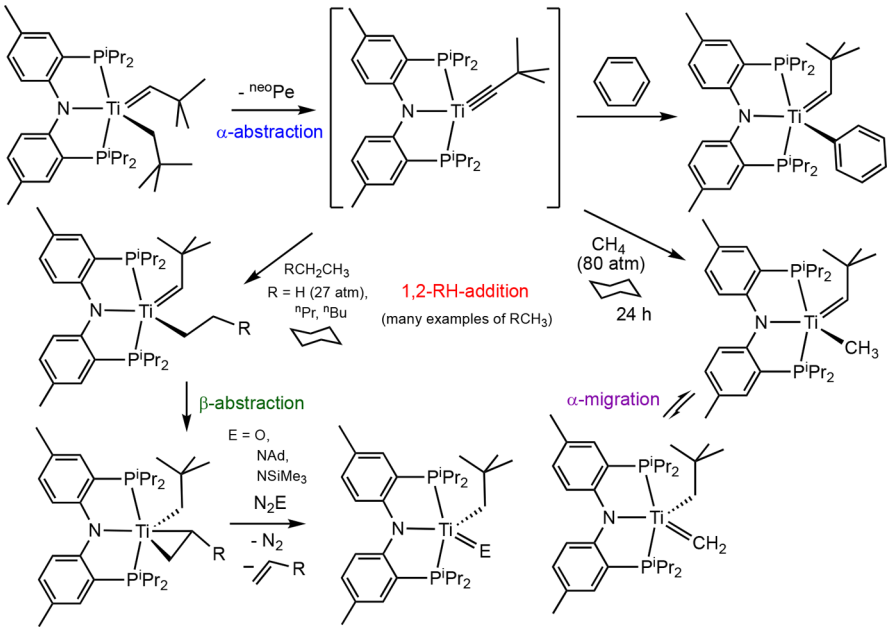




DOI: 10.1021/acs.organomet.7b00753
Organometallics 2018, 37, 505−516

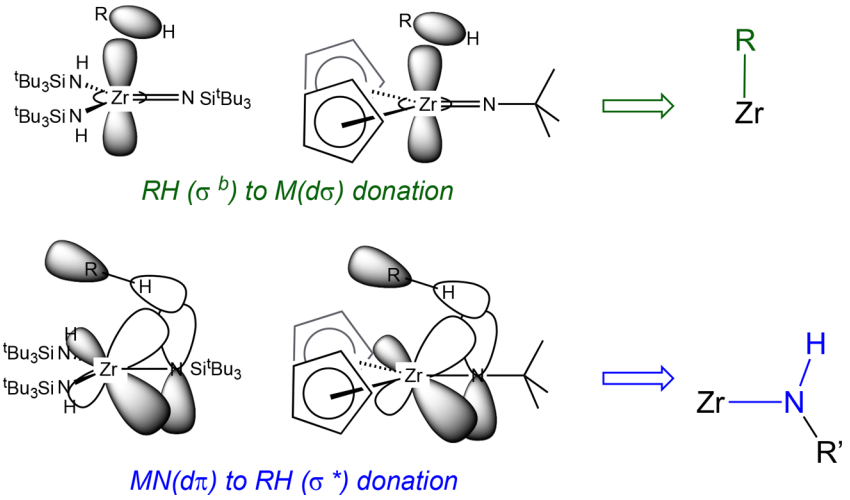


**Figure 1.** View of the localized electrophilic site, essentially an empty $d_{z^2}$ orbital, on the transient imides $(^tBu_3SiNH)_2Zr{=}NSi^tBu_3$ (**2**) and $Cp_2Zr{=}N^tBu$ (**5**), showing the initial interaction with a hydrocarbon, RH. Bond breaking ultimately occurs via donation from metal-imido electron density into the RH ($\sigma^*$) orbital. Both interactions are crucial to the generation of the ZrR and NH bonds.

**Scheme 4. General Mechanism for 1,2-RH-Elimination/-Addition to Transient Early Metal Imides**

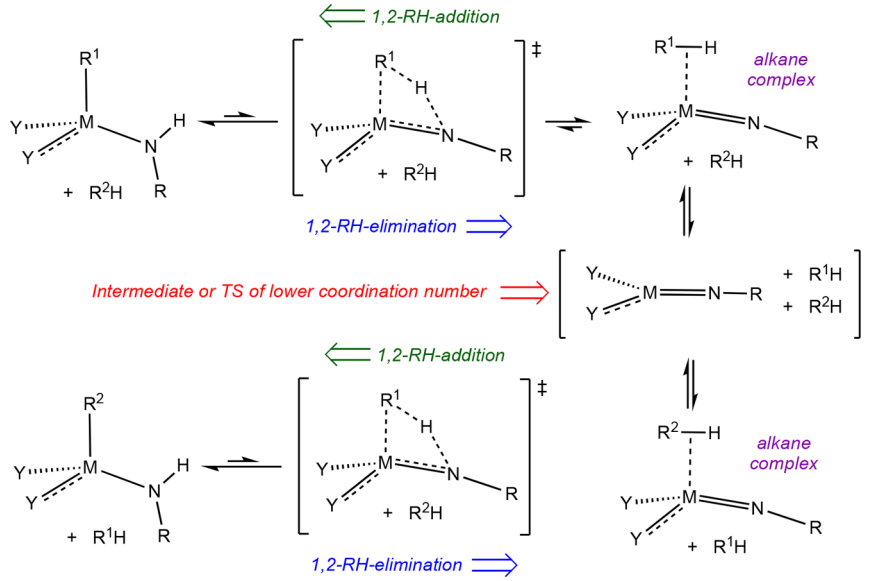


imide nitrogen leads to productive 1,2-RH-addition. Two factors contribute to the regiochemistry of addition: (1) Sterics favor R addition to the metal over the more crowded nitrogen. (2) The spherical symmetry of the hydrogen 1s orbital[25−28] renders it able to overlap with two atoms without significant reorganizational energy. The latter factor is likely the most important, as the migrationof H between two atoms in $\alpha$-[29] and $\beta$-H-elimination/insertion[30] events, and $\sigma$-bond metathesis[31,32] has this commonality.

The basicity accorded the metal−imide bond, polarized $M(\delta^+)-N(\delta^-)$, serves to interact with the RH $\sigma^*$ orbital to accept the proton and generate the NH bond. Concomitant with amide bond formation, the empty $M(d\sigma)$ orbital interacts with the RH electron density to ultimately become the M−R bond. Attempts to correlate RH activation events with hydrocarbon acidities were not particularly informative; thus, it is best to consider the electrophilic activation of the RH bond and its ultimate disruption as occurring in concert. Calculations also support the separate interactions as occurring within a concerted four-center TS.

**General Mechanism.** While the key orbital interactions of the hydrocarbon occur with the transient imides $(^tBu_3SiNH)_2Zr{=}NSi^tBu_3$ (**2**) and $Cp_2Zr{=}N^tBu$ (**5**), in neither system are these intermediates directly observed. Focusing on the amide systems, Scheme 4 illustrates the overall process for CH-bond activation, which includes the microscopic reverse of the activation process, 1,2-RH-elimination. Amide alkyls of group 4, $(^tBu_3SiNH)_3MR$ (M = Ti, R = Me, **7**-Me;[33] M = Zr, **1**-R;[1,3,34] M = Hf, R = Me, **8**-Me) and $(silox)_2(^tBu_3SiNH)TiR$ (**9**-R, silox = $^tBu_3SiO$),[35,36] as well as related imide-amide alkyls of group 5 $(^tBu_3SiNH)_2(^tBu_3SiN{=})MR$ (M = V,[37] **10**-R; Ta, **11**-R),[38] have all displayed 1,2-RH-elimination reactivity that can be rationalized as generating pseudotrigonal imido species that can add C−H bonds in a reverse 1,2-RH-addition process. The 1,2-RH-elimination in the group 5 cases requires greater thermal energy than that in the group 4 complexes within their


DOI: 10.1021/acs.organomet.7b00753
Organometallics 2018, 37, 505−516

**Table 1. Ground State $\Delta G°$ Values of $(silox)_2(^tBu_3SiNH)TiR$ (9-R) and $(silox)_2(^tBu_3SiN{=})TiL$ (14-L) and Activation Energies ($\Delta G^‡$) for RH Loss from 9-R Relative to $(silox)_2(^tBu_3SiN{=})Tipy$ (14-py) at $\Delta G_{rel}°(24.8°C)$ = 0.0 kcal/mol[a]**

| cmpd[b] | $T$ (±0.3,°C) | $\Delta G°_{rel}$(GS) (kcal/mol) | $k_{elim}$ (× $10^5$) ($s^{-1}$) | $\Delta G^‡$ (kcal/mol) | BDE (kcal/mol) |
|---|---|---|---|---|---|
| $X_2(^tBu_3SiNH)Ti^cHex$ (9-$^c$Hex) | 24.8 | 19.1 | 8.8(6) | 23.0 | 99.5 |
| | 24.8[c] | 18.2 | 4.6(2) | 23.4 | 95.6 |
| | 40.4[c] | | 25(2) | 23.6 | |
| $X_2(^tBu_3SiNH)Ti^cPe$ (9-$^c$Pe) | 50.5[c] | | 70(1) | 23.7 | |
| | 60.0[c] | | 174(4) | 23.8 | |
| | 70.9[c] | | 434(12) | 24.0 | |
| $X_2(^tBu_3SiNH)Ti^nBu$ (9-$^n$Bu) | 24.8 | 16.9 | 2.05(3) | 23.8 | 100.7 |
| $X_2(^tBu_3SiNH)TiCH_2CH_2{}^tBu$ (9-$^{neo}$Hex) | 24.8 | 16.8 | 1.71(8) | 23.9 | 100.2 |
| $X_2(^tBu_3SiNH)TiEt$ (9-Et) | 24.8 | 16.5 | 1.86(10) | 23.9 | 100.5 |
| $X_2(^tBu_3SiNH)Ti^cBu$ (9-$^c$Bu) | 24.8 | 16.4 | 2.13(8) | 23.8 | 96.8 |
| $X_2(^tBu_3SiNH)TiPh$ (9-Ph)[d] | 24.8 | 15.6 | 33.3(3) | 22.2 | 112.9 |
| $X_2(^tBu_3SiND)TiPh$ (9-ND-Ph)[d] | 24.8 | | 6.7(8) | 23.1 | |
| | 24.8[e] | 14.7 | 1.54(10) | 24.0 | 105.0 |
| | 35.1[e] | | 4.9(7) | 24.1 | |
| $X_2(^tBu_3SiNH)TiMe$ (9-Me) | 50.2[e] | | 30(2) | 24.2 | |
| | 63.6[e] | | 79(6) | 24.6 | |
| | 71.3[e] | | 170(20) | 24.6 | |
| $X_2(^tBu_3SiNH)TiMe$ (9-Me)[f] | 24.8 | | 1.54(7) | 24.0 | |
| $X_2(^tBu_3SiND)TiMe$ (9-ND-Me)[f] | 24.8 | | 0.112(6) | 25.6 | |
| | 24.8[g] | 14.6 | 0.086(6) | 25.7 | 88.5 |
| $X_2(^tBu_3SiNH)TiCH_2Ph$ (9-Bn) | 52.4[g,h] | | 2.26(5) | 26.0 | |
| | 70.2[g,h] | | 17(1) | 26.1 | |
| | 90.2[g,h] | | 92(2) | 26.5 | |
| | 52.4[h] | | 0.21(1) | 27.6 | |
| $X_2(^tBu_3SiND)TiCH_2Ph$ (9-ND-Bn) | 70.2[h] | | 1.80(5) | 27.6 | |
| | 90.2[h] | | 16.3(5) | 27.7 | |
| $X_2(^tBu_3SiNH)Ti^cPr$ (9-$^c$Pr) | 24.8 | 13.8 | 2.13 | 23.8 | 106.3 |
| $X_2(^tBu_3SiNH)TiCH_2(C_6H_3\text{-}3,5\text{-}Me_2)$ (9-Mes) | 24.8 | 13.8 | 0.0872 | 25.7 | 88.5 |
| $X_2(^tBu_3SiNH)TiCH{=}CH_2$ (9-Vy) | 24.8 | 13.6 | 23.9 | 22.4 | 111.2 |
| $X_2(^tBu_3SiNH)TiH$ (9-H) | 24.8 | 8.6 | 0.58 | 24.6 | 104.2 |
| $X_2(^tBu_3SiN{=})Ti(THF)$ (14-THF) | 24.8 | 3.4 | | | |
| $X_2(^tBu_3SiN{=})Tipy$ (14-py) | 24.8 | 0.0 | | | |

[a]Kinetics runs done in triplicate in $C_6D_6$ to produce $(silox)_2(^tBu_3SiND)Ti(C_6D_5)$ (9-ND-$C_6D_5$) unless otherwise noted. [b](X = silox = $^tBu_3SiO$). [c]From an Eyring plot, using a weighted, nonlinear least-squares fit of the data: $\Delta H^‡$ = 19.6(6) kcal/mol; $\Delta S^‡$ = −13(2) eu. [d]Runs done in tandem afforded $k_H/k_D$ = 4.9(8). [e]From an Eyring plot, using a weighted, nonlinear least-squares fit of the data: $\Delta H^‡$ = 20.2(12) kcal/mol; $\Delta S^‡$ = −12(4) eu. [f]Runs done in tandem in $C_6D_{12}$ with 20 equiv of THF (product 14-THF) afforded $k_H/k_D$ = 13.7(9). [g]From an Eyring plot, using a weighted, nonlinear least-squares fit of the data: $\Delta H^‡$ = 22.2(5) kcal/mol; $\Delta S^‡$ = −12(2) eu. [h]Runs done in tandem afforded $k_H/k_D$ = 10.8(8) at 52.4 °C, 9.4(9) at 70.2 °C, and 5.6(3) at 90.2 °C.

respective rows, and corresponding tungsten complexes $(^tBu_3SiNH)(^tBu_3SiN{=})_2WR$ (12-R)[39−41] are remarkably stable and manifest no elimination.

The elimination/addition reaction occurs via a 4-centered TS reminiscent of transition metal $\sigma$-bond metathesis reactions studied by Bercaw et al. in the late 1980s.[31] While substantial data has been generated on the 1,2-RH-elimination reaction, the 1,2-RH-addition complement has only been inferred from product analyses and equilibrium studies, since no stable metal imide has been subjected to alkanes and observed to add C−H bonds. Alkane complexes are also likely intermediates in the forward and reverse reactions, and these have been vetted by calculation.[24] In many transformations involving reactive low-coordinate intermediates, the proposed three-coordinate imide may only exist in alkane bound form. For example, in related tungsten chemistry, reactivity consistent with the generation of $(^tBu_3SiN{=})_3W(RH)$ (13-RH) leads to the production of $(^tBu_3SiNH)(^tBu_3SiN{=})_2WR$ (12-R).[39,40]

**Kinetics of 1,2-RH-Elimination.** The most comprehensive and informative set of data related to CH-bond activation via 1,2-RH-elimination/-addition is found in the $(silox)_2(^tBu_3SiNH)TiR$ (9-R)[35,36] system, where equilibria of the type given in eq 1 permits an assessment of crucial relative ground-state (GS) energies.

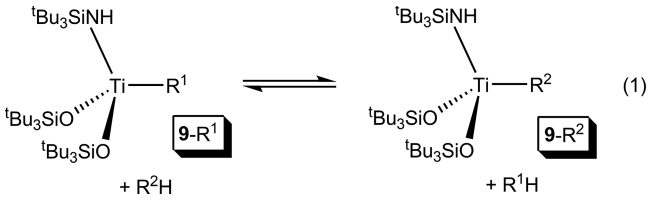

(1)

The GS energies relative to $(silox)_2(^tBu_3SiN{=})Tipy$ (14-py) and corresponding transition state (TS) energies for 1,2-RH-elimination of 9-R are listed in Table 1 and are expressed as a columnar chart in Figure 2. Activation free energies were obtained for the $^c$Pe−H, Me−H, and $PhCH_2$−H loss from the corresponding alkyls, and the values are consistent with a fairly constrained geometry for elimination, as $\Delta S^‡$ is around −12 eu for all three cases. For the remainder of the discussion, it will be assumed that activation entropies are similar for all 1,2-RH-elimination cases.



DOI: 10.1021/acs.organomet.7b00753
Organometallics 2018, 37, 505−516

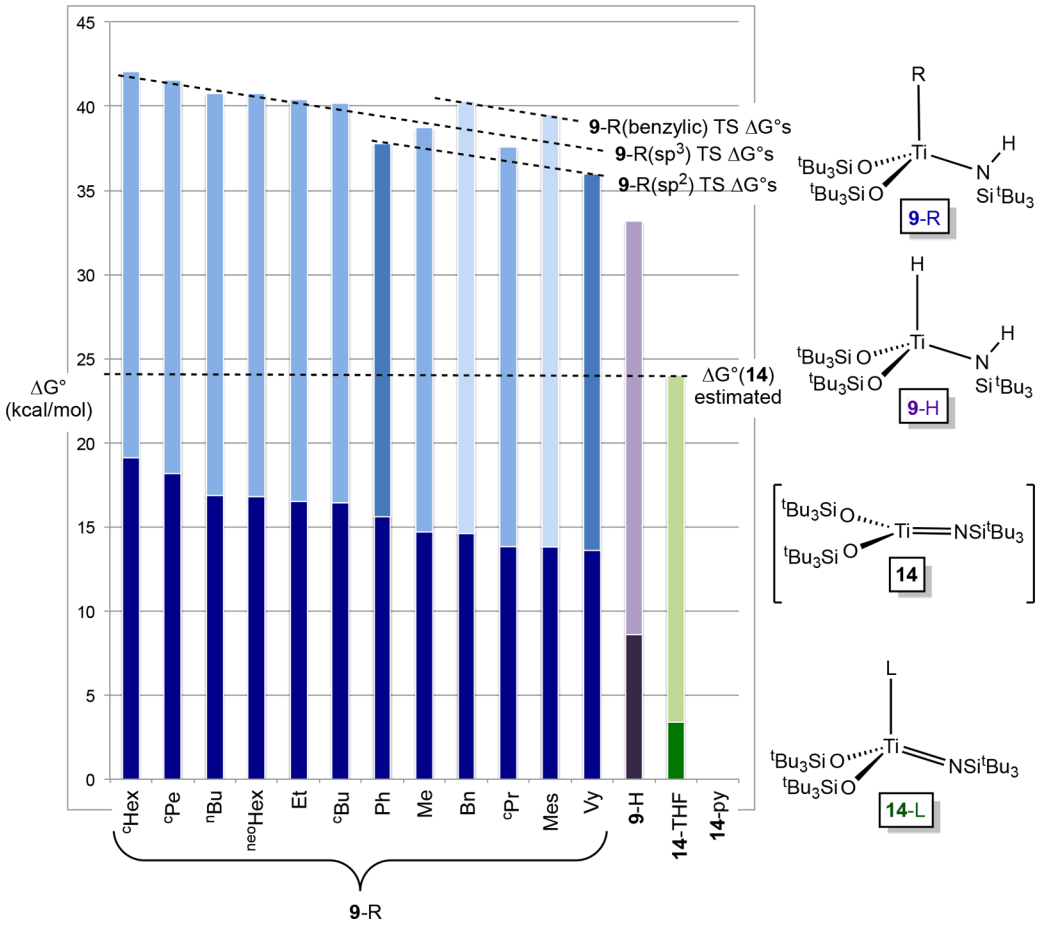


**Figure 2.** Standard free energies, $\Delta G^\circ$, pertaining to ground states of (silox)$_2$($^t$Bu$_3$NH)TiR (**9**-R, R = hydrocarbyl, H), and (silox)$_2$($^t$Bu$_3$N═)TiL (**14**-L), relative to those of (silox)$_2$($^t$Bu$_3$N═)Tipy (**14**-py) at 0.0 kcal/mol (dark columns). The lighter columns refer to $\Delta G^{\ddagger}_{elim}$ from **9**-R and TS energies, obtained by $\Delta G^\circ$(GS) + $\Delta G^{\ddagger}_{elim}$, are given by the tops of the columns.

Three major factors contribute to the free energies of the TSs leading to (silox)$_2$($^t$Bu$_3$SiNH)TiR (**9**-R). As is clear from Figure 2, there is a linear free energy (LFE) relationship, since the general slope of the TS standard free energies tracks with those of the GSs. Second, as is indicated by the dashed lines in the chart, sp$^3$ eliminations are separate from sp$^2$ substituents, and benzylic substrates represent a third set. In order to understand the transition-state free energy factors, the GS energy differences must be evaluated in view of the aforementioned relationship. Temperature-dependent equilibrium measurements and analyses of statistical factors suggested that $\Delta S^\circ$ was essentially unimportant in determining the $\Delta G^\circ_{rel}$(GS) values listed in Table 1; hence, the equilibria of eq 1 can be represented as differences in bond dissociation enthalpies (BDEs) of R$^1$H versus R$^2$H and D(TiR$^1$) versus D(TiR$^2$) according to the following:[42]

$$\Delta G^\circ_{rxn} \sim \Delta H^\circ_{rxn} \sim [D(TiR^1) - D(TiR^2)] + [D(R^2H) - D(R^1H)] \quad (2)$$

$$[D(TiR^1) - D(TiR^2)] = D(TiR)_{rel} \sim \Delta H^\circ_{rxn} - [D(R^2H) - D(R^1H)] \quad (3)$$

As BDEs of hydrocarbons have been reassessed since the initial publication of this data,[43] some modest changes in the relationship are apparent, but the differences in D(RH) values are essentially compensated by the differences in relative titanium−carbon bond energies, as Figure 3 illustrates. Often, the ΔD(MR) are greater than the ΔD(HR),[44−47] but in this case, there is not much difference. Subtle variations in the $\beta$ pertaining to ΔD(TiR) = $\beta${ΔD(HR)} can be found depending on the values used for the hydrocarbon BDEs.

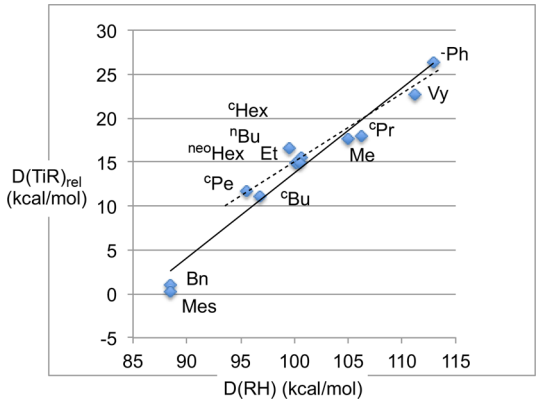


**Figure 3.** Plot showing that the differences in D(R$^1$H) vs D(R$^2$H) in eq 1 are roughly compensated by differences in D(TiR$^2$) vs D(TiR$^1$). The slope is $\beta$ = 0.97, and the $R^2$ value is 0.946. Elimination of the benzylic cases (dashed line) affords a slope of $\beta$ = 0.77 ($R^2$ = 0.933).

An assessment of 1,2-RH-elimination/-addition can now be conducted with three-coordinate (silox)$_2$Ti═NSi$^t$Bu$_3$ (**14**) as



DOI: 10.1021/acs.organomet.7b00753
Organometallics 2018, 37, 505−516

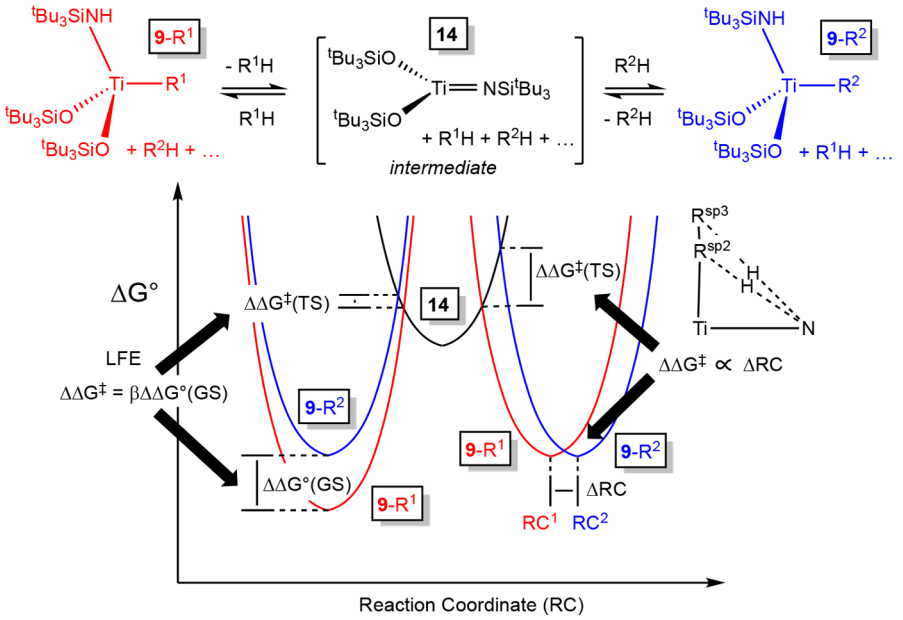


**Figure 4.** 1,2-RH-elimination/-addition is illustrated via $R^1H$ or $R^2H$ addition to (silox)$_2$Ti═NSi$^t$Bu$_3$ (**14**). The generation of (silox)$_2$($^t$Bu$_3$SiNH)Ti$R^1$ (**9**-$R^1$, red) or **9**-$R^2$ (blue) is dependent on two crucial factors: (1) the linear free energy (LFE) relationship upon addition and (2) compression or elongation of the reaction coordinate (RC), right.

the proposed intermediate, providing an Occam's razor pathway for understanding the reaction. Rates of THF loss from (silox)$_2$($^t$Bu$_3$SiN═)Ti(THF) (**14**-THF) and the inability to detect any elimination product by NMR spectroscopy in thermolyses of (silox)$_2$($^t$Bu$_3$SiNH)Ti$^c$Hex (**9**-$^c$Hex) led to an estimate of ~24 kcal/mol for the $\Delta G^\circ$ of **14** (relative to **14**-py at 0.0 kcal/mol). As a consequence, $\Delta G^{\ddagger}_{addn}$ values can be estimated as $\Delta G^\circ$(TS) − 24 kcal/mol, thereby revealing selectivities for RH activation, which will be discussed later.

As Figure 4 reveals, basic enthalpic features of the reaction can be readily understood, since $\Delta\Delta H^\circ \sim \Delta\Delta G^\circ$ as explained above. Assume **14** has been generated, and two substrates are available for 1,2-RH-addition, $R^1H$ and $R^2H$. The activation energy for the formation of **9**-$R^1$ is less than that of **9**-$R^2$ because there is an enthalpic preference for $R^1H$ activation over $R^2H$, i.e., $\Delta G^\circ$(**9**-$R^1$) < $\Delta G^\circ$(**9**-$R^2$). This is seen in the Figure 5 plot of $\Delta G^{\ddagger}_{addn}$ versus $\Delta G^\circ$(**9**-R), which clearly reveals this linear free energy (LFE) relationship. In essence, as long as the reaction coordinates for RH-activation are similar, the reaction is driven by the strength of the Ti−R bond formed. Note that this is opposite to free radical or hydrogen atom transfer (HAT) activations, in which the weaker CH bonds are activated selectively.[46−49] LFE also predicts that the $\Delta G^{\ddagger}_{elim}$ values for similar substrates should be alike; for example, the average $\Delta G^{\ddagger}_{elim}$ is 23.7(3) kcal/mol for all sp$^3$-substrates except benzylics.

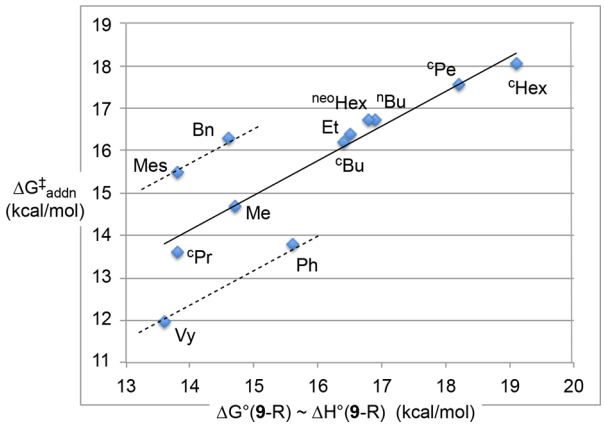


**Figure 5.** 1,2-RH-addition activation energies ($\Delta G^{\ddagger}_{addn}$) of RH by (silox)$_2$Ti═NSi$^t$Bu$_3$ (**14**) are shown to correlate with the stabilities ($\Delta G^\circ$(**9**-R), Figure 4, LFE) of (silox)$_2$($^t$Bu$_3$SiNH)TiR (**9**-R), with corrections due to compression of the RC (**9**-Vy, **9**-Ph, Figure 4), and inductive effects (**9**-Bn, **9**-Mes; see text).

The second most important factor in determining activation selectivities, i.e., $\Delta\Delta G^{\ddagger}_{addn}$, is the reaction coordinate (RC). Assuming similar enthalpies of reaction for $R^1H$ versus $R^2H$ (Figure 4), $\Delta G^\circ$(**9**-$R^1$) is equal to $\Delta G^\circ$(**9**-$R^2$); hence, there should be no selectivity by argument of the linear free energy relationship. If the RC were more compressed for activation of $R^1H$ ($RC^1$) than $R^2H$ ($RC^2$), then the TS for generation of **9**-$R^1$ is considerably lower. This is the case for sp$^2$-substrates PhH and VyH, and Figure 5 shows these to be displaced relative to the sp$^3$-set of substrates, indicating swifter activation. The RC is compressed, as illustrated for sp$^3$ versus sp$^2$, because the latter $d$(TiC) are shorter; hence, the 1,2-R(sp$^2$)H-addition occurs in a more compact TS. Implicit in these arguments is that the potential energy (or free energy) wells corresponding to (silox)$_2$($^t$Bu$_3$SiNH)TiR (**9**-R) each have the same steepness, i.e., the shape of the parabolas are similar, a reasonable assumption given the likely bond strengths of the titanium−carbon bonds in the system.[42]

Neither of the two factors exhibited in Figure 5 explains why the sp$^3$-benzylic compounds, (silox)$_2$($^t$Bu$_3$SiNH)TiBn (**9**-Bn) and (silox)$_2$($^t$Bu$_3$SiNH)TiCH$_2$(3,5-Me$_2$-C$_6$H$_3$) (**9**-Mes), are skewed from the sp$^3$-line of substrates. What is likely, and what has been shown to contribute in d$^8$ RH-oxidative additions,[45] is an inductive effect by the phenyl group on the bound carbon in a metal-benzyl bond. Having an sp$^2$-substituent on the $\alpha$-carbon, with its slightly higher electronegativity, increases the ionic character of the metal−carbon


DOI: 10.1021/acs.organomet.7b00753
Organometallics 2018, 37, 505−516

**Table 2. Measured and Estimated Rates, $\Delta G^{\ddagger}_{elim}$, and $k_{rel}$ for 1,2-RH-Elimination from Group 4 and 5 XY($^t$Bu$_3$SiNH)MR Complexes**

| group 4 compound | $(10^5)k$ ($s^{-1}$) (kcal/mol)[a] | $\Delta G^{\ddagger}_{elim}$ | $k_{rel}$ | group 5 compound | $(10^5)k$ ($s^{-1}$) (kcal/mol)[a] | $\Delta G^{\ddagger}_{elim}$ | $k_{rel}$ |
|---|---|---|---|---|---|---|---|
| (silox)$_2$($^t$Bu$_3$SiNH)TiMe (**9**-Me) | 2120 | 24.6 | 600 | ($^t$Bu$_3$SiNH)$_2$($^t$Bu$_3$SiN)VMe (**10**-Me)[b] | 37.7 | 27.6 | 10.6 |
| (silox)$_2$($^t$Bu$_3$SiNH)TiPh (**9**-Ph) | 18600 | 23.0 | 5270 | ($^t$Bu$_3$SiNH)$_2$($^t$Bu$_3$SiN)VPh (**10**-Ph)[b,c] | 437 | 25.8 | 124 |
| ($^t$Bu$_3$SiNH)$_3$ZrMe (**1**-Me) | 3.53 | 29.9 | 1 | | | | |
| ($^t$Bu$_3$SiNH)$_3$ZrPh (**1**-Ph) | 753 | 25.4 | 21 | | | | |
| ($^t$Bu$_3$SiNH)$_3$HfMe[b,d] (**8**-Me) | 0.00706 | 33.9 | 0.0020 | ($^t$Bu$_3$SiNH)$_2$($^t$Bu$_3$SiN)TaMe (**11**-Me)[b] | $6.1 \times 10^{-5}$ | 37.4 | $2 \times 10^{-5}$ |
| ($^t$Bu$_3$SiNH)$_3$HfPh[b] (**8**-Ph) | 1.51 | 30.0 | 0.43 | ($^t$Bu$_3$SiNH)$_2$($^t$Bu$_3$SiN)TaPh (**11**-Ph)[b] | $2.4 \times 10^{-3}$ | 34.7 | $7 \times 10^{-4}$ |

[a]Rate constants were recalculated/estimated at 96.7 °C and corrected for the number of NH units per molecule. [b]$\Delta S^{\ddagger}$ assumed to be −10 eu. [c]$k_{Ph}/k_{Me}$ assumed to be similar to that of the zirconium case. [d]$k_{Ph}/k_{Me}$ assumed to be similar to that of the tantalum case.

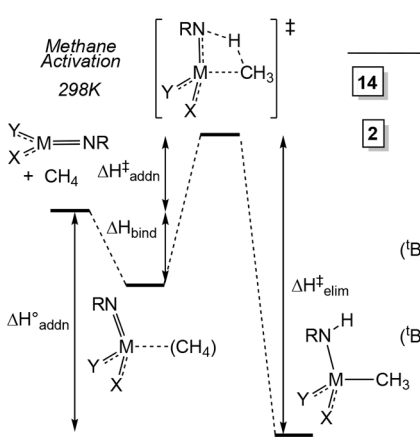


| | Cmpd (exp) XYM=NSi$^t$Bu$_3$ | Cmpd (calcd) XYM=NH | ΔH°addn | ΔH°bind | ΔH‡addn | ΔH‡elim |
|---|---|---|---|---|---|---|
| | | | (kcal/mol) | | | |
| 14 | ($^t$Bu$_3$SiO)$_2$Ti=NSi$^t$Bu$_3$ | | -7.5 | | *12.7 (20)* | 20.2 (12) |
| | | (HO)$_2$Ti=NH | -8.9 | -4.0 | 14.4 | 23.3 |
| 2 | ($^t$Bu$_3$SiNH)$_2$Zr=NSi$^t$Bu$_3$ | | | | *11 (8)* | 25.9 (4) |
| | | (H$_2$N)$_2$Zr=NH | -21.7 | -6.0 | 12.2 | 33.9 |
| | ($^t$Bu$_3$SiNH)$_2$Hf=NSi$^t$Bu$_3$ | | | | | 30.3 |
| | | (H$_2$N)$_2$Hf=NH | -33.4 | -8.6 | 4.9 | 38.3 |
| | ($^t$Bu$_3$SiNH)(($^t$Bu$_3$SiN)V=NSi$^t$Bu$_3$ | | | | | 23.9 |
| | | (H$_2$N)(HN)V=NH | -18.5 | -13.2 | 5.1 | 23.6 |
| | | (H$_2$N)(HN)Nb=NH | -28.5 | -11.1 | 10.1 | 38.6 |
| | ($^t$Bu$_3$SiNH)(($^t$Bu$_3$SiN)Ta=NSi$^t$Bu$_3$ | | | | | 33.7 |
| | | (H$_2$N)(HN)Ta=NH | -39.8 | -13.1 | 3.1 | 42.9 |
| | | (HN)$_2$Mo=NH | -48.4 | -13.7 | 7.4 | 55.8 |
| | | (HN)$_2$W=NH | -60.3 | -15.6 | 1.3 | 61.6 |

**Figure 6.** Experimental (blue) and calculated (red) 1,2-MeH-elimination and -addition activation enthalpies, and enthapies of MeH binding and addition to metal imidos of groups 4−6 at 298 K (experimental estimates in *italics*). In the calculations, the $^t$Bu$_3$Si group has been replaced with H.

bond, thereby rendering its bond strength greater than expected and lowering the $\Delta G°$(GS) values for **9**-Bn and **9**-Mes. The inductive effect is less influential in the TS ($\Delta G°$(TS)); hence, the activations of BnH and MesH occur at higher energies than expected. Inductive effects have proven important in a variety of CH bond activations, even hydrogen atom abstractions (HAT), where $CH_3CN$ (BDE = 96 kcal/mol) and $Cl_2CH_2$ (BDE = 97.3 kcal/mol) are often solvents for complexes that undergo HAT with substrates having stronger CH bonds.[46−49] The factors affecting RH bond activation for (silox)$_2$($^t$Bu$_3$SiNH)TiR (**9**-R) appear general for other imide CH-bond activation systems, but modest $\Delta G°$(GS) information for ($^t$Bu$_3$SiNH)$_3$ZrR (**1**-R)[3,34] and only relative rate information for a limited number of activations by Cp*CpZr═N$^t$Bu hamper detailed interpretation.[50,51]

**Periodic Trends in 1,2-RH-elimination.** Table 2 lists estimates of 1,2-MeH and 1,2-PhH-elimination rates and activation free energies for (silox)$_2$($^t$Bu$_3$SiNH)TiR (**9**-R),[35] ($^t$Bu$_3$SiNH)$_3$MR (M = Zr, **1**-R;[34] Hf, **8**-R),[35] and ($^t$Bu$_3$SiNH)$_2$($^t$Bu$_3$SiN)MR (M = V,[37] **10**-R; Ta, **11**-R).[38] There is a rough decline of 4−5 kcal/mol in $\Delta G^{\ddagger}_{elim}$ per row in group 4, and while there are no Nb examples for group 5, the difference between V and Ta implicates similar changes. In moving from group 4 to 5, an increase in ∼3−4 kcal/mol occurs for each column, and the related 1,2-RH-elimination from ($^t$Bu$_3$SiNH)($^t$Bu$_3$SiN═)$_2$WR (**12**-R),[39−41] as the only representative from group 6, has not been realized.

TSs for MeH activation by the second row transition metal three-coordinate imides are calculated to be slightly higher than those of their first or third row congeners for groups 5 and 6,[23,41] but otherwise the trends exhibited in Figure 6 are as expected. A more favorable $\Delta H°_{addn}$ is calculated upon descent of a column, presumably due to exchange of a MN $\pi$-bond for N−H and M−Me $\sigma$-bonds, since the latter are likely to increase in strength. It is also plausible that the energy of the transient imido species, e.g., **2**, **14**, etc., rises down a group due to increasing diffusivity of the d-orbitals.

The $\Delta H°_{addn}$ values get progressively larger, in the range of ∼20 kcal/mol, upon descending a column within each group, but the magnitudes of $\Delta H°_{addn}$ increase substantially from group 4 to 6, culminating in a huge $\Delta H°_{addn}$(calc) = −60.3 kcal/mol for MeH activation by (HN═)W, affording (HN)(HN═)WMe (**12**-Me).[39,40] While (HN═)$_3$W may be construed as an 18e$^-$ complex, assuming each imide contributes 6e$^-$ as a dianion and is therefore less prone to react with RH, the calculations suggest the opposite. First, the complex is not an 18e$^-$ species, as one pair of electrons to the *tris*-imido set of ligands is intrinsically nonbonding due to a mismatch in symmetry.[52] Second, the competition for efficient utilization of the d-orbitals by competing $\pi$-donor ligands weakens the $\pi$-bonds from group 4 to 5 to 6, and the transient pseudotrigonal species become progressively higher in energy.[52−54]

As Figure 6 indicates, activation energy calculations of 1,2-MeH-elimination are generally in line with the experimentally determined, directly or indirectly, data of MeH loss from the XY($^t$Bu$_3$SiNH)MMe systems, although they err to the high side. Although calculations suggested that 1,2-MeH-elimination from ($^t$Bu$_3$SiNH)($^t$Bu$_3$SiN═)$_2$WMe (**12**-Me) was prohibitive at $\Delta H^{\ddagger}_{elim}$ = 61.6 kcal/mol, the tungsten system was still interesting due to a significant enthalpy of methane binding of −15.6 kcal/mol to ($^t$Bu$_3$SiN═)$_3$W (**13**); even the free energy of MeH binding was favorable at $\Delta G°_{bind}$ = −8.4 kcal/


DOI: 10.1021/acs.organomet.7b00753
*Organometallics* 2018, 37, 505−516

**Scheme 5. Indirect Evidence of Alkane Complexes ($^t$Bu$_3$SiN═)$_3$W (13-RH) via Hydride Transfer from ($^t$Bu$_3$SiN═)$_3$W(HK) (13-HK) to RX**

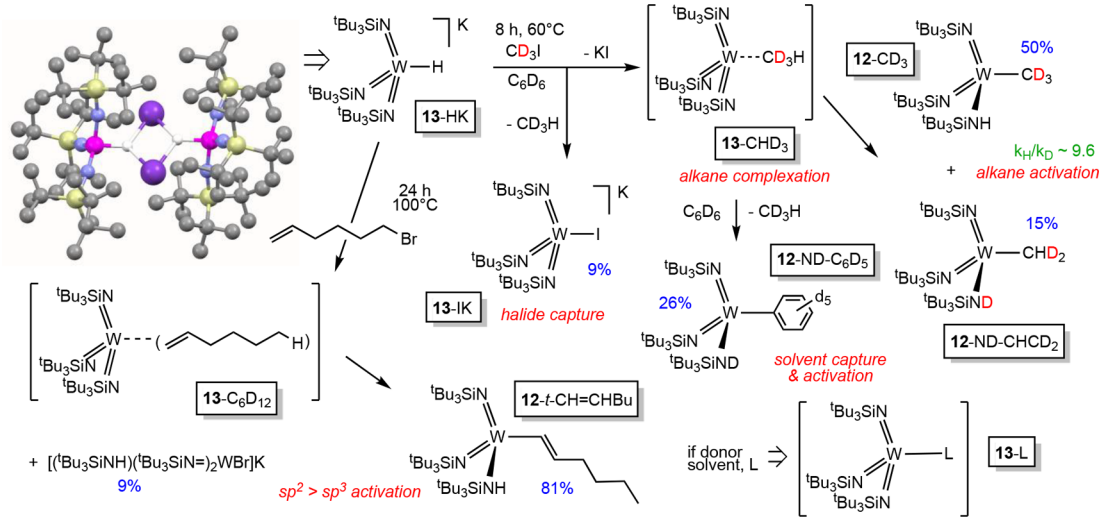


mol.[23,24,41] Three-coordinate imido species were also pyramidalized in the second and third rows in groups 5 and 6 due to $n$ $d_{z^2}/(n + 1)$p/$(n + 1)$s mixing,[55−58] a geometric distortion favorable toward binding.

**Alkane Complexes: A More Complex Activation Mechanism.** The Occam's razor approach in Figure 4 has enabled a satisfactory explanation for much of the energy differences pertaining to the various substrates undergoing 1,2-RH-addition to the early transition metal imidos and the reverse 1,2-RH-eliminations from the related alkyl species. Calculations (Figure 6) suggest that additional intermediates between pseudo trigonal XYM═NSi$^t$Bu$_3$ (+RH) and the activation products XY($^t$Bu$_3$SiNH)MR are alkane-bound species, XY($^t$Bu$_3$SiN═)M(RH).[24,41] Alkane complex intermediates are unlikely to change the arguments above unless their formation is the rate-determining event in CH bond activation. As the calculations in Figure 6 suggest, the RH-complexes (and the barriers to formation) are smaller than the barriers to activation of RH in these systems, which contrast with $d^8$ CH-bond oxidative additions where the barriers to alkane binding determine the hydrocarbon activation selectivities.[59,60]

Scheme 5 illustrates a means to generate and obtain indirect evidence of alkane complexes in the tungsten system. The potassium hydride adduct of ($^t$Bu$_3$SiN═)$_3$W (**13**) exists as a dimer in crystalline form, [($^t$Bu$_3$SiN═)$_3$W]$_2$(H($\mu$-K)$_2$H) (**13**-HK)$_2$,[41] in which the potassium cations are each coordinated to two hydrides and loosely affiliated with a host of CH bonds from the $^t$Bu groups. In solution, **13**-HK serves as a hydride donor when exposed to alkyl-halides. For example, treatment of **13**-HK with $CD_3I$ affords three products, iodide adduct [($^t$Bu$_3$SiN═)$_3$WI]K (**13**-IK),[39,40] benzene ($C_6D_6$)-activated aryl complex ($^t$Bu$_3$SiND)($^t$Bu$_3$SiN═)$_2$W$C_6D_5$ (**12**-ND-$C_6D_5$), and two products derived from the activation of $CHD_3$: ($^t$Bu$_3$SiNH)($^t$Bu$_3$SiN═)$_2$W$CD_3$ (**12**-$CD_3$) and ($^t$Bu$_3$SiND)-($^t$Bu$_3$SiN═)$_2$W$CHD_2$ (**12**-ND-$CHD_2$). The ratio of the latter products, once statistics are taken into account, provides a $k_H/k_D$ for $CHD_3$ activation of ~9.6 at 60 °C. The products are consistent with hydride displacement of iodide from $CD_3I$ and scavenging of either primary product, KI or $CHD_3$, by ($^t$Bu$_3$SiN═)$_3$W (**13**) to generate **13**-IK and ($^t$Bu$_3$SiN═)$_3$W-($CHD_3$) (**13**-$CHD_3$). The methane complex can lose $CHD_3$ and activate $C_6D_6$ solvent to afford **12**-ND-$C_6D_5$ or undergo 1,2-RH/D-addition to provide **12**-$CD_3$ and **12**-ND-$CHD_2$.

Exploration of a various reactions of [($^t$Bu$_3$SiN═)$_3$W]$_2$(H-($\mu$-K)$_2$H) (**13**-HK) with halocarbons reveals 1,2-RH-addition chemistry derived from MeX and unhindered primary substrates (RX, R = Et, Pr, etc.), and for benzylic and vinylic halides.[40] For benzylic halides, products (**12**-R) containing aryl− and benzyl−tungsten bonds are produced in ratios consistent with the aforementioned preference for aryl−H activation, sterics, and the appropriate statistics. A related, pertinent example is the reaction of **13**-HK with 5-hexenyl-bromide illustrated in Scheme 5. Simple hydride delivery would generate 1-hexene bound to tungsten, i.e., ($^t$Bu$_3$SiN═)$_3$W-($C_6H_{12}$) (**13**-$C_6H_{12}$), but the ultimate product is ($^t$Bu$_3$SiNH)-($^t$Bu$_3$SiN═)$_2$W(*trans*-CH═CH$^n$Bu) (**12**-*t*-CH═CH$^n$Bu), revealing CH-activation solely at the *trans*-vinylic position, as expected from substrate preferences (Figure 2). All of the halocarbon reactivity with **13**-HK can be rationalized via the intermediacy of hydrocarbon complexes, and product distributions of $R^HX$ versus $R^DX$ substrates can be used to determine crude alkane binding inverse isotope effects that suggest $CH_4$ is slightly more strongly bound than $CHD_3$ ($k_H/k_D = z \sim 0.94$), and $C_2H_6$ is bound more tightly than $CH_3CD_3$ ($z \sim 0.89$).

**Kinetic Isotope Effects on 1,2-RH-Elimination and -Addition.** Kinetic isotope effects (KIEs; $k_H/k_D = z$) for 1,2-RH-elimination ($k_H$(elim)/$k_D$(elim) = $z_{elim}$) have been measured for (silox)$_2$($^t$Bu$_3$SiNH/D)TiR (R = Me, **9**-Me (**9**-ND-Me), $z_{elim}$ = 13.7(9) at 24.8 °C; $CH_2$Ph, **9**-Bn (**9**-(ND)-Bn), $z_{elim}$ = 10.8(8) at 52.4 °C, 9.4(9) at 70.2 °C, 5.6(3) at 90.2 °C; Ph, **9**-Ph (**9**-ND-Ph), $z_{elim}$ = 5.0(8) at 24.8 °C,[35] ($^t$Bu$_3$SiNH/D)$_3$ZrR (R = Me, **1**-Me (**1**-ND-Me), $z_{elim}$ = 6.27(8) at 96.7 °C; **1**-Bn (**1**-(ND)-Bn), $z_{elim}$ = 7.1(6) at 96.8 °C; Ph, **1**-Ph (**1**-ND-Ph), $z_{elim}$ = 4.6(4) at 96.7 °C,[34] and ($^t$Bu$_3$SiNH/D)$_2$($^t$Bu$_3$SiN═)TaMe (**11**-Me (**11**-ND-Me)), $z_{elim}$ = 3.4(9) at 182.8 °C.[38] Despite being three independent systems and three metals, there is a reasonable temperature dependence on the $z_{elim}$ values for sp$^3$-alkyls ($z_{elim}$ = −0.0644($T$(K)) + 31.291 with $R^2$ = 0.84), suggesting a commonality of mechanism, and similar reaction coordinates for each. The large values for sp$^3$-substrates implicate a reaction



DOI: 10.1021/acs.organomet.7b00753
*Organometallics* 2018, 37, 505−516

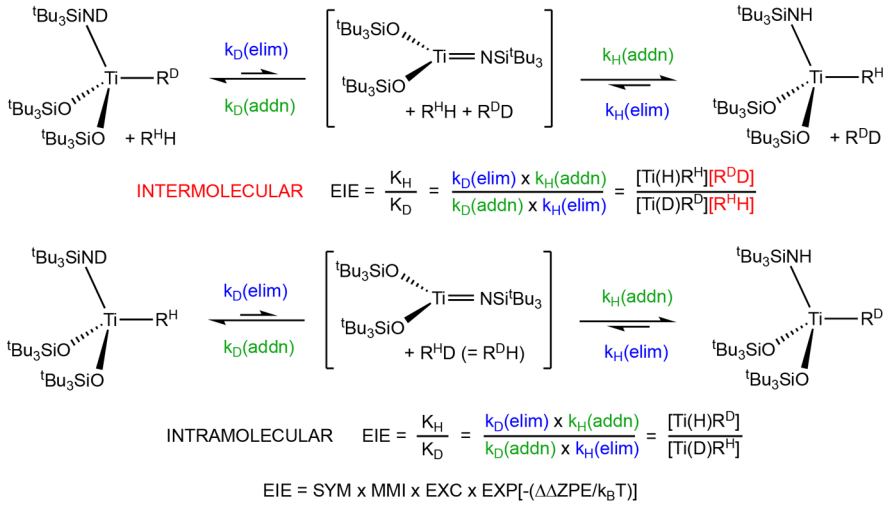


| $R^HH/R^DD$ | $R^DH = R^HD$ | $EIE_{obs}$/SYM | $EIE_{calc}$/SYM | $KIE_{elim}$ | $KIE_{addn}$(exp) | $KIE_{addn}$(calc) |
|---|---|---|---|---|---|---|
| $CH_4/CD_4$ | | 2.00 (6) | 1.88 | 14.7 (17) | 29.4 (35) | 27.6 |
| | $CDH_3$ | 1.05 (8) | 0.87 | 13.4 (10) | 14.1 (15) | 11.7 |
| | $CD_2H_2$ | 1.13 (8) | 0.91 | | 15.1 (16) | 12.2 |
| | $CD_3H$ | 1.17 (7) | 0.91 | | 15.7 (15) | 12.2 |
| $C_2H_6/C_2D_6$ | | 2.22 (8) | 1.93 | 14.3 (7) | 31.7 (19) | 27.6 |
| | $CD_3CH_3$ | 1.53 (3) | 1.44 | | 21.9 (12) | 20.6 |

**Figure 7.** Intermolecular ($R^HH$ vs $R^DD$) and intramolecular ($R^HD{=}R^DH$) equilibrium and kinetic isotope effects (EIEs, KIEs) determined at 24.8 °C for the $(silox)_2(^tBu_3SiN(H/D))Ti(R^D/R^H)$ system. $KIE_{elim}$ (blue) are measured. The $KIE_{addn}$ were generated using experimental EIEs ($KIE_{addn}(exp) = EIE_{obs}/KIE_{elim}$) or calculated EIEs ($KIE_{addn}(calc) = EIE_{calc}/KIE_{elim}$). SYM refers to statistical effects that are factored out as indicated. Consult the primary references for the functional forms of the EIE or KIE expressions.

coordinate for H-transfer that is neither particularly early nor late. It is plausible that phenyl, and by analogy, vinylic substituents, have a less balanced reaction coordinate, given their lower $z_{elim}$.

The generation of alkane complexes, $(^tBu_3SiN{=})_3W(RH)$ (**13**-RH), has permitted measurement of KIEs for 1,2-RH-addition ($k_H(addn)/k_D(addn) = z_{addn}$) via the ratio of $(^tBu_3SiNH)(^tBu_3SiN{=})_2WR^D$ (**12**-$R^D$) and $(^tBu_3SiND)(^tBu_3SiN{=})_2WCHD_2$ (**12**-ND-$R^H$) products: RH = $HCD_3$, solvent = $C_6D_6$, 60 °C, $z_{addn}$ = 9.6(6); RH = $HCD_3$, solvent = $Et_2O$, 60 °C, $z_{addn}$ = 9.9(6), RH = $HCD_3$, solvent = THF, 100 °C, $z_{addn}$ = 11.7(6), RH = $CH_3CD_3$, solvent = $C_6D_6$, 100 °C, $z_{addn}$ = 7.9(3). As explained above, these KIEs also contain an alkane binding equilibrium isotope effect (EIE) and secondary effects, but they are likely near 1 and will not change the KIEs outside of their error in measurement. Bergman's hydrocarbon additions to transiently generated Cp*CpZr=N$^t$Bu provide another set of 1,2-RH-addition KIEs: benzene-$d_0$/-$d_6$, $z_{addn}$ = 7.4; $^n$PeH-$d_0$/-$d_{12}$, $z_{addn}$ = 8.9; mesitylene-$d_0$/-$d_{12}$, $z_{addn}$ = 8.8; $^t$BuCH$_2$–*trans*-HC=CH(H/D), $z_{addn}$ = 6.9.[50] The magnitudes of the 1,2-RH-addition KIEs are roughly equivalent to the elimination KIEs, supporting the claim of a balanced H-transfer in the TS.

Information obtained from KIE experiments is typically limited to the confirmation of rate-determining steps and interpretations of early or late TSs. In one system, that of hydrocarbon activations by $(silox)_2Ti{=}NSi^tBu_3$ (**14**),[61] the combination of EIEs and KIEs has enabled a deeper understanding of the activation events. Figure 7 delineates the intra- and intermolecular experiments conducted, and numbers obtained from measurements of EIEs and KIEs on selected examples involving methane and ethane.

In the intermolecular measurement of an EIE, the perprotiated alkyl, $(silox)_2(^tBu_3NH)TiR^H$ (**9**-$R^H$), was integrated versus the substrate $R^HH$ in the $^1$H NMR spectrum, and the corresponding perdeuterated complex, $(silox)_2(^tBu_3ND)$-$TiR^D$ (**9**-ND-$R^D$), and substrate $R^DD$ were integrated in the $^2$H NMR spectrum. The two ratios were multiplied to achieve the EIE, and since the EIE ($K_H/K_D$) as written is the ratio of KIEs($z_{addn}/z_{elim}$), $z_{addn}$ can be determined from measurements of EIE and $z_{elim}$, i.e., $z_{addn} = (EIE)(z_{elim})$. Note the difference between the intermolecular EIE and the intramolecular KIE. In the intermolecular EIE, the expression contains the ratio of protio and deuterio substrates, but the intramolecular EIE equation does not contain the substrate. The difference has important consequences on the interpretation of KIEs, which also can be differentiated on this basis.

Consider the $KIE_{addn}$ values of 29.4(35) (calc 27.6) obtained for the intermolecular experiment involving $CH_4$ versus $CD_4$ activation. The values are extraordinary, perhaps inviting an unusual interpretation, such as quantum mechanical tunneling. The intramolecular values for $KIE_{addn}$, obtained from $H_3CD$ (14.1(15)), $H_2CD_2$ (15.1(16)), and $HCD_3$ (15.7(15)), are essentially half that of the intermolecular case. There is no reason why the activation of $H_{3-n}CD_n$ should be fundamentally different than activation of $CH_4$ versus $CD_4$, and examination of the data reveals the EIE measurement is the source of the factor of 2. The difference in EIEs stems from the necessity to assess the difference in energy content of the substrates. The ratio of $[CD_4]/[CH_4]$, due to differences in translation, rotation (MMI), population of excited vibrational levels (excitation, EXC), and zero point energies (ZPE), is a factor of 2, and it has nothing to do with a CH versus CD 1,2-addition event. The experimental differences are significantly manifested when



DOI: 10.1021/acs.organomet.7b00753
*Organometallics* 2018, 37, 505–516

substrates of low mass are involved, as can be readily seen in the $CH_4/CD_4$ versus $CH_nD_{4-n}$ ($n$ = 1−3) and $C_2H_6/C_2D_6$ versus ($CH_3CD_3$) examples in Figure 7; for examples of larger mass, consult the primary source.[61]

Although the magnitudes of the KIEs for both elimination and addition appear high, this is a consequence of using organic systems as the context for comparison. Organic compounds, and corresponding reactions, possess a limited range of vibrations in which energy is deposited, largely due to their strong CH bonds.[62−65] Typical vibrational frequencies in an organic compound range from 3300 to 700 $cm^{-1}$, whereas transition metal compounds can often have much lower frequency vibrations (approaching 100 $cm^{-1}$ and lower), usually oscillators that couple to the metal in varying amounts. The softer potential wells harboring such vibrations have the net effect of making the excitation and ZPE terms contribute more in organometallic complexes, causing greater variation and substantially greater magnitudes in observed EIEs and KIEs. While it is possible that quantum mechanical tunneling contributes to the large KIEs, classical explanations of KIEs are normally sufficient to explain the magnitudes.[61]

**Selectivities in CH-Activation.** The differences in TS energies illustrated in Figure 2 reveal that ∼6 kcal/mol in hydrocarbon selectivity is available in the $(silox)_2Ti{=}NSi^tBu_3$ (**14**) system.[35] Using the TS energies, i.e., adding the $\Delta G^\circ_{rel}$ and $\Delta G^\ddagger$ for each species in Table 1, affords the following selectivities in CH bond activation relative to $H_2$ activation, the easiest (24.8 °C, kcal/mol): $H_2$ (0.0) > Vy−H (2.8) > $^c$Pr−H (3.4) > Ph−H (4.6) > Me−H (5.5) > Mes−H (6.3) > $^c$BuH (7.0) > Bn−H (7.1) > Et−H (7.2) > $^{neo}$Hex−H (7.5) > $^n$Bu−H (7.5) > $^c$PeH (8.4) > $^c$Hex−H (8.9). The selectivities reflect the general trend for concerted activations, i.e.,[46] ones that do not follow free radical or related paths: $sp^2$-substrates ∼ cyclopropane > $sp^3$-primary alkanes > $sp^3$-cyclic alkanes. Variation in the activation of benzylic and allylic bonds has been noted. For systems that activate CH bonds via oxidative addition, such as $d^8$ species that are coordinatively unsaturated,[59,60] the differences in TS energies are <2 kcal/mol at similar temperatures, because alkane (C−H bond) binding is the selectivity determining step.

While the energy values separating the 1,2-RH-addition TSs for the various hydrocarbon substrates are modest, they provide hope for the direct conversion of alkanes to functionalized, i.e., oxidized products. For example, methane is more easily activated than ethane, evidence that methane homologation systems can be realized. In addition, the deactivation of CH bonds via inductive effects, as exhibited by the relatively slow activation of benzylic substrates, suggests that oxidized hydrocarbons may be stable to overoxidation, which is the greatest problem facing conversion of commodity hydrocarbons. In radical CH activation systems, such as in autoxidation, the initial activation event typically renders products more susceptible to further oxidation.

**Future Directions.** Fundamentals of 1,2-RH-addition and 1,2-RH-elimination have been generally elucidated, but practical application subsequent to the activation event, i.e., functionalization of the hydrocarbon, has thus far not been realized for early transition metal imides. It is conceivable that 1,2-RH-activation can be coupled with alkylidene or olefin insertion chemistry, thereby providing a pathway for homologation of hydrocarbons, but the discovery of a suitable system has yet to occur. It may be that related 1,2-activation chemistry, such as that of olefins, may hold the greatest promise for applications. For a selection of versatile reactivity, consult the work Bergman et al. on the activation of allenes,[66] additions of epoxide,[67] the catalytic hydroamination of alkynes,[68] and related 2 + 2 reactions.[69,70] For an additional perspective on early transition metal imido chemistry, the work of Mountford et al. deserves attention.[71,72]

## AUTHOR INFORMATION


### Corresponding Author

*E-mail: ptw2@cornell.edu.

### ORCID

Peter T. Wolczanski: 0000-0003-4801-0614


### Notes

The author declares no competing financial interest.

## ACKNOWLEDGMENTS


Support from the National Science Foundation (CHE-1402149; CHE-1664580) and Cornell University is gratefully acknowledged. In the P.T.W. group, the discovery of 1,2-RH-elimination/-addition is attributed to Christopher "Kit" Cummins, with help from Steven M. Baxter. Exhaustive studies on Zr and Ta by Christopher P. Schaller led to the Ti study of greatest scope, which was conducted by Jordan L. (Bennett) Fantini. EIE and KIE measurements were painstakingly conducted by Lee M. Slaughter, and Dan F. Schafer II elucidated the role of hydrocarbon complexes in tunsten-hydride delivery to RX. Thanks to the R.G.B. group, especially Patrick J. Walsh, at University of California, Berkeley, for sharing our experiences in 1,2-RH-activation. Calculations were critical to many of the general interpretations, and a special thank you is given to Thomas R. Cundari for a fruitful 28+ year collaboration, much of which was spent on the analysis of 1,2-RH-elimination/-addition.


## REFERENCES


(1) Cummins, C. C.; Wolczanski, P. T. *Abstr. Papers Am. Chem. Soc.* **1988**, *195*, 738.

(2) Walsh, P. J.; Bergman, R. G. *Abstr. Papers Am. Chem. Soc.* **1988**, *195*, 490.

(3) Cummins, C. C.; Baxter, S. M.; Wolczanski, P. T. *J. Am. Chem. Soc.* **1988**, *110*, 8731−8733.

(4) Walsh, P. J.; Hollander, F. J.; Bergman, R. G. *J. Am. Chem. Soc.* **1988**, *110*, 8729−8731.

(5) Schrock, R. R.; Coperet, C. *Organometallics* **2017**, *36*, 1884−1892.

(6) (a) Schrock, R. R. *Chem. Rev.* **2002**, *102*, 145−179. (b) Schrock, R. R.; Hoveyda, A. H. *Angew. Chem., Int. Ed.* **2003**, *42*, 4592−4633.

(7) (a) Abbott, J. K. C.; Li, L.; Xue, Z.-L. *J. Am. Chem. Soc.* **2009**, *131*, 8246−8251. (b) Xue, Z.-L.; Morton, L. A. *J. Organomet. Chem.* **2011**, *696*, 3924−3934. (c) Morton, L. A.; Chen, S. J.; Qiu, H.; Xue, Z.-L. *J. Am. Chem. Soc.* **2007**, *129*, 7277−7283. (d) Dougan, B. A.; Xue, Z.-L. *Organometallics* **2009**, *28*, 1295−1302.

(8) (a) McDade, C.; Green, J. C.; Bercaw, J. E. *Organometallics* **1982**, *1*, 1629−1634. (b) Bulls, A. R.; Schaefer, W. P.; Serfas, M.; Bercaw, J. E. *Organometallics* **1987**, *6*, 1219−1226.

(9) (a) van Doorn, J. A.; van der Heijden, H.; Orpen, A. G. *Organometallics* **1994**, *13*, 4271−4277. (b) van Doorn, J. A.; van der Heijden, H.; Orpen, A. G. *Organometallics* **1995**, *14*, 1278−1283.

(10) (a) Chamberlain, L. R.; Rothwell, I. P.; Huffman, J. C. *J. Am. Chem. Soc.* **1986**, *108*, 1502−1509. (b) Vilardo, J. S.; Lockwood, M. A.; Hanson, L. G.; Clark, J. R.; Parkin, B. C.; Fanwick, P. E.; Rothwell, I. P. *J. Chem. Soc., Dalton Trans.* **1997**, *1997*, 3353−3362.

(11) Plundrich, G. T.; Wadepohl, H.; Gade, L. H. *Inorg. Chem.* **2016**, *55*, 353−365.




DOI: 10.1021/acs.organomet.7b00753
*Organometallics* 2018, 37, 505−516

(12) (a) van der Heijden, H.; Hessen, B. *J. Chem. Soc., Chem. Commun.* **1995**, 145−146. (b) van der Heijden, H.; Hessen, B. *Inorg. Chim. Acta* **2003**, *345*, 27−36. (c) Deckers, P. J. W.; Hessen, B. *Organometallics* **2002**, *21*, 5564−5575.
(13) Zhang, S.; Tamm, M.; Nomura, K. *Organometallics* **2011**, *30*, 2712−2720.
(14) Andino, J. G.; Kilgore, U. J.; Pink, M.; Ozarowski, A.; Krzystek, J.; Telser, J.; Baik, M.-H.; Mindiola, D. J. *Chem. Sci.* **2010**, *1*, 351−356.
(15) (a) Wada, K.; Pamplin, C. B.; Legzdins, P.; Patrick, B. O.; Tsyba, I.; Bau, R. *J. Am. Chem. Soc.* **2003**, *125*, 7035−7048. (b) Adams, C. S.; Legzdins, P.; Tran, E. *Organometallics* **2002**, *21*, 1474−1486. (c) Pamplin, C. B.; Legzdins, P. *Acc. Chem. Res.* **2003**, *36*, 223−233.
(16) Cheon, J.; Rogers, D. M.; Girolami, G. S. *J. Am. Chem. Soc.* **1997**, *119*, 6804−6813.
(17) Cavaliere, V. N.; Mindiola, D. J. *Chem. Sci.* **2012**, *3*, 3356−3365.
(18) (a) Bailey, B. C.; Fan, H.; Huffman, J. C.; Baik, M.-H.; Mindiola, D. J. *J. Am. Chem. Soc.* **2007**, *129*, 8781−8793. (b) Bailey, B. C.; Fan, H.; Baum, E. W.; Huffman, J. C.; Baik, M.-H.; Mindiola, D. J. *J. Am. Chem. Soc.* **2005**, *127*, 16016−16017.
(19) (a) Crestani, M. G.; Hickey, A. K.; Gao, X. F.; PInter, B.; Cavaliere, V. N.; Ito, J.-I.; Chen, C. H.; Mindiola, D. J. *J. Am. Chem. Soc.* **2013**, *135*, 14754−14767. (b) Cavaliere, V. N.; Crestani, M. G.; Pinter, B.; Pink, M.; Chen, C.-H.; Baik, M.-H.; Mindiola, D. J. *J. Am. Chem. Soc.* **2011**, *133*, 10700−10703.
(20) Flores, J. A.; Cavaliere, V. N.; Buck, D.; Pinter, B.; Chen, G.; Crestani, M. G.; Baik, M.-H.; Mindiola, D. J. *Chem. Sci.* **2011**, *2*, 1457−1462.
(21) (a) Fan, H.; Fout, A. R.; Bailey, B. C.; Pink, M.; Baik, M.-H.; Mindiola, D. J. *Dalton Trans.* **2013**, *42*, 4163−4174. (b) Kurogi, T.; Carroll, P. J.; Mindiola, D. J. *Chem. Commun.* **2017**, *53*, 3412−3414.
(22) (a) Green, M. L. H.; Parkin, G. *J. Chem. Educ.* **2014**, *91*, 807−816. (b) Parkin, G. *J. Chem. Educ.* **2006**, *83*, 791−799. (c) Green, M. L. H. *J. Organomet. Chem.* **1995**, *500*, 127−148.
(23) (a) Cundari, T. R. *J. Am. Chem. Soc.* **1992**, *114*, 10557−10563. (b) Cundari, T. R. *Organometallics* **1993**, *12*, 4971−4978. (c) Cundari, T. R. *Organometallics* **1994**, *13*, 2987−2994. (d) Cundari, T. R.; Curtiss, S. *Int. J. Quantum Chem.* **1996**, *60*, 779−788. (e) Benson, M. T.; Bryan, J. C.; Burrell, A. K.; Cundari, T. R. *Inorg. Chem.* **1995**, *34*, 2348−2355. (f) Cundari, T. R.; Matsunaga, N.; Moody, E. W. *J. Phys. Chem.* **1996**, *100*, 6475−6483. (g) Cundari, T. R.; Klinckman, T. R. *Inorg. Chem.* **1998**, *37*, 5399−5401.
(24) Cundari, T. R.; Klinckman, T. R.; Wolczanski, P. T. *J. Am. Chem. Soc.* **2002**, *124*, 1481−1487.
(25) Lauher, J. W.; Hoffmann, R. *J. Am. Chem. Soc.* **1976**, *98*, 1729−1742.
(26) Fujimoto, H.; Yamasaki, T.; Mizutani, H.; Koga, N. *J. Am. Chem. Soc.* **1985**, *107*, 6157−6161.
(27) Han, Y.; Deng, L.; Ziegler, T. *J. Am. Chem. Soc.* **1997**, *119*, 5939−5945.
(28) Prosenc, M.-H.; Janiak, C.; Brintzinger, H.-H. *Organometallics* **1992**, *11*, 4036−4041.
(29) Threlkel, R. S.; Bercaw, J. E. *J. Am. Chem. Soc.* **1981**, *103*, 2650−2659.
(30) Doherty, N. M.; Bercaw, J. E. *J. Am. Chem. Soc.* **1985**, *107*, 2670−2682.
(31) Thompson, M. E.; Baxter, S. M.; Bulls, A. R.; Burger, B. J.; Nolan, M. C.; Santarsiero, B. D.; Schaefer, W. P.; Bercaw, J. E. *J. Am. Chem. Soc.* **1987**, *109*, 203−219.
(32) Tilley, T. D. *Acc. Chem. Res.* **1993**, *26*, 22−29.
(33) Cummins, C. C.; Schaller, C. P.; Van Duyne, G. D.; Wolczanski, P. T.; Chan, E.A.-W.; Hoffmann, R. *J. Am. Chem. Soc.* **1991**, *113*, 2985−2994.
(34) Schaller, C. P.; Cummins, C. C.; Wolczanski, P. T. *J. Am. Chem. Soc.* **1996**, *118*, 591−611.
(35) Bennett, J. L.; Wolczanski, P. T. *J. Am. Chem. Soc.* **1997**, *119*, 10696−10719.
(36) Bennett, J. L.; Wolczanski, P. T. *J. Am. Chem. Soc.* **1994**, *116*, 2179−2180.
(37) de With, J.; Horton, A. D. *Angew. Chem., Int. Ed. Engl.* **1993**, *32*, 903−905.
(38) Schaller, C. P.; Wolczanski, P. T. *Inorg. Chem.* **1993**, *32*, 131−144.
(39) Schafer, D. F., II; Wolczanski, P. T. *J. Am. Chem. Soc.* **1998**, *120*, 4881−4882.
(40) Schafer, D. F., II; Wolczanski, P. T.; Lobkovsky, E. B. *Organometallics* **2011**, *30*, 6518−6538.
(41) Schafer, D. F., II; Wolczanski, P. T.; Lobkovsky, E. B. *Organometallics* **2011**, *30*, 6539−6561.
(42) Bennett, J. L.; Vaid, T. P.; Wolczanski, P. T. *Inorg. Chim. Acta* **1998**, *270*, 414−423.
(43) Luo, Y.-R., Ed. *Handbook of Bond Dissociation Energies in Organic Compounds*; CRC Press: New York, 2003.
(44) Bryndza, H. E.; Fong, L. K.; Paciello, R. A.; Tam, W.; Bercaw, J. E. J. *J. Am. Chem. Soc.* **1987**, *109*, 1444−1456.
(45) Jiao, Y.; Evans, M. E.; Morris, J.; Brennessel, W. W.; Jones, W. D. *J. Am. Chem. Soc.* **2013**, *135*, 6994−7004.
(46) Crabtree, R. H.; Lei, A. W. *Chem. Rev.* **2017**, *117*, 8481−8482.
(47) Xue, X.-S.; Ji, P.; Zhou, B.; Cheng, J.-P. *Chem. Rev.* **2017**, *117*, 8622−8648.
(48) (a) Saouma, C. T.; Mayer, J. M. *Chem. Sci.* **2014**, *5*, 21−31. (b) Mayer, J. M. *Acc. Chem. Res.* **2011**, *44*, 36−46. (c) Mayer, J. M. *Acc. Chem. Res.* **1998**, *31*, 441−450.
(49) Sydora, O. L.; Goldsmith, J. I.; Vaid, T. P.; Miller, A. E.; Wolczanski, P. T.; Abruña, H. D. *Polyhedron* **2004**, *23*, 2841−2856.
(50) Hoyt, H. M.; Bergman, R. G. *Angew. Chem., Int. Ed.* **2007**, *46*, 5580−5582.
(51) Hoyt, H. M.; Michael, F. E.; Bergman, R. G. *J. Am. Chem. Soc.* **2004**, *126*, 1018−1019.
(52) (a) Anhaus, J. T.; Kee, T. P.; Schofield, M. H.; Schrock, R. R. *J. Am. Chem. Soc.* **1990**, *112*, 1642−1643. (b) Schofield, M. H.; Kee, T. P.; Anhaus, J. T.; Schrock, R. R.; Johnson, K. H.; Davis, W. M. *Inorg. Chem.* **1991**, *30*, 3595−3604.
(53) (a) Morrison, D. L.; Rodgers, P. M.; Chao, Y.-W.; Bruck, M. A.; Grittini, C.; Tajima, T. L.; Alexander, S. J.; Rheingold, A. L.; Wigley, D. E. *Organometallics* **1995**, *14*, 2435−2446. (b) Chao, Y. W.; Rodgers, P. M.; Wigley, D. E.; Alexander, S. J.; Rheingold, A. L. *J. Am. Chem. Soc.* **1991**, *113*, 6326−6328. (c) Morrison, D. L.; Wigley, D. E. *Inorg. Chem.* **1995**, *34*, 2610−2616.
(54) Wigley, D. E. *Prog. Inorg. Chem.* **1994**, *42*, 239−482.
(55) Hirsekorn, K. F.; Hulley, E. B.; Wolczanski, P. T.; Cundari, T. R. *J. Am. Chem. Soc.* **2008**, *130*, 1183−1196.
(56) Kuiper, D. S.; Douthwaite, R. E.; Mayol, A.-R.; Wolczanski, P. T.; Lobkovsky, E. B.; Cundari, T. R.; Lam, O. P.; Meyer, K. *Inorg. Chem.* **2008**, *47*, 7139−7153.
(57) Kuiper, D. S.; Wolczanski, P. T.; Lobkovsky, E. B.; Cundari, T. R. *J. Am. Chem. Soc.* **2008**, *130*, 12931−12943.
(58) Kuiper, D. S.; Wolczanski, P. T.; Lobkovsky, E. B.; Cundari, T. R. *Inorg. Chem.* **2008**, *47*, 10542−10553.
(59) Jones, W. D.; Hessell, E. T. *J. Am. Chem. Soc.* **1993**, *115*, 554−562.
(60) Periana, R. A.; Bergman, R. G. *J. Am. Chem. Soc.* **1986**, *108*, 7332−7346.
(61) Slaughter, L. M.; Wolczanski, P. T.; Klinckman, T. R.; Cundari, T. R. *J. Am. Chem. Soc.* **2000**, *122*, 7953−7975.
(62) Carpenter, B. K. *Determination of Reaction Mechanisms*; Wiley-Interscience: New York, 1984.
(63) Melander, L.; Saunders, W. H., Jr. *Reaction Rates of Isotopic Molecules*; Wiley-Interscience: New York, 1980.
(64) Collins, C. J., Bowman, N. S., Eds. *Isotope Effects in Chemical Reactions*; ACS Monograph No. 167; Van Nostrand Reinhold Co.: New York, 1970.
(65) Westheimer, F. H. *Chem. Rev.* **1961**, *61*, 265−273.
(66) (a) Michael, F. E.; Duncan, A. P.; Sweeney, Z. K.; Bergman, R. G. *J. Am. Chem. Soc.* **2003**, *125*, 7184−7185. (b) Michael, F. E.; Duncan, A. P.; Sweeney, Z. K.; Bergman, R. G. *J. Am. Chem. Soc.* **2005**, *127*, 1752−1764.


DOI: 10.1021/acs.organomet.7b00753
*Organometallics* 2018, 37, 505−516

(67) (a) Blum, S. A.; Walsh, P. J.; Bergman, R. G. *J. Am. Chem. Soc.* **2003**, *125*, 14276−14277;(b) **2004**, *126*, 9148. (correction of ref 67a). (c) Blum, S. A.; Rivera, V. A.; Ruck, R. T.; Michael, F. E.; Bergman, R. G. *Organometallics* **2005**, *24*, 1647−1659.
(68) (a) Walsh, P. J.; Baranger, A. M.; Bergman, R. G. *J. Am. Chem. Soc.* **1992**, *114*, 1708−1719. (b) Baranger, A. M.; Walsh, P. J.; Bergman, R. G. *J. Am. Chem. Soc.* **1993**, *115*, 2753−2763.
(69) (a) Meyer, K. E.; Walsh, P. J.; Bergman, R. G. *J. Am. Chem. Soc.* **1994**, *116*, 2669−2670. (b) Meyer, K. E.; Walsh, P. J.; Bergman, R. G. *J. Am. Chem. Soc.* **1995**, *117*, 974−985.
(70) Walsh, P. J.; Hollander, F. J.; Bergman, R. G. *Organometallics* **1993**, *12*, 3705−3723.
(71) Schwarz, A. D.; Nielson, A. J.; Kaltsoyannis, N.; Mountford, P. *Chem. Sci.* **2012**, *3*, 819−824.
(72) Hazari, N.; Mountford, P. *Acc. Chem. Res.* **2005**, *38*, 839−849.



DOI: 10.1021/acs.organomet.7b00753
*Organometallics* 2018, 37, 505−516